Chemistry–A European Journal

Research Article
doi.org/10.1002/chem.202203636

Chemistry Europe
European Chemical Societies Publishing

www.chemeurj.org

Liquid Dynamics Determine Transition Metal-*N*-Heterocyclic Carbene Complex Formation

Paul Zaby,[a] Jan Blasius,[a] Anna K. Müller,[a] Steven P. Nolan,[b] and Oldamur Hollóczki*[c]

Abstract: The mechanism of metal-*N*-heterocyclic carbene (NHC) complex formation from imidazolium salts in the presence of weak bases was investigated through theoretical methods. Quantum chemical calculations revealed that the two bases considered here, sodium acetate and trimethylamine, both facilitate complex formation. In contrast to previous experiments, these calculations indicated a slightly lower barrier with the amine. Molecular dynamics simulations showed that the ionic nature of the $[AuCl_2]^-$ and imidazolium ions, as well as the sodium acetate base keep these species associated in the reaction mixture through ion pairing. This pre-association of the components produces those clusters that are essential for the metal complex formation reaction. The neutral amine, however, remains mostly separated from the other reaction partners, making it a significantly less effective base.

Introduction

N-Heterocyclic carbenes (NHCs) are widely used as ligands in transition metal catalysis, enabling efficient routes for organic synthesis.[1–4] The preparation of these complexes from the metal compound and the azolium cation has been based on four main methods. In the "free carbene route" (Figure 1A), the azolium cation is first deprotonated by a strong base to form a free NHC, followed by the reaction of this species with the metal to form the desired complex.[5–9] While this reaction has a general applicability, it suffers from the inefficient and costly handling of aggressive bases and the reactive free carbene under inert atmosphere. Another route is transmetalation (Figure 1B), which relies on the direct reaction of a metal oxide with the azolium cation, forming a carbene complex in a single step, and subsequently the exchange of the metal to another.[6,10–12] This approach avoids some drawbacks of the free carbene route, but its scope is limited to copper and silver derivatives, while it usually requires harsh conditions. In some cases, a third strategy, the "built-in base route" was found successful (Figure 1C), in which the metal complex bears a basic ligand (e.g. acetylacetonate), facilitating the deprotonation of the imidazolium ring, and the formation of the complex.[13,14] An interesting version of this method is using imidazolium acetate,[15–17] chloride,[17] or hydrogen carbonate[18] ionic liquids as carbene precursors, with the counterion of the imidazolium cation acting as base. In these cases, however, the introduction of the base into the starting materials must be possible, whereas the resulting compound must have a low melting point, which significantly limit the applicability of this approach.

In the 2010s, the "weak base route" emerged (Figure 1D),[19–21] offering an alternative to the either somewhat limited or inefficient synthetic methods. In these procedures, azolium salts are brought into reaction with metal sources in

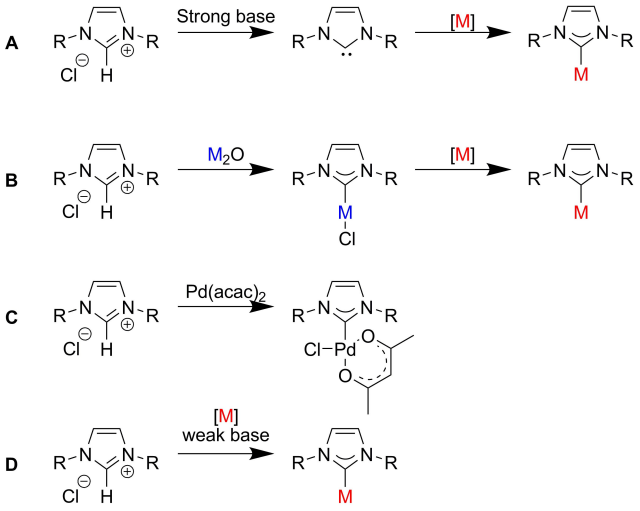

Figure 1. Synthetic methods leading to transition metal-NHC complexes (A: free carbene route; B: transmetalation route; C: built-in base route; D: weak base route).[19]

[a] *P. Zaby, J. Blasius, A. K. Müller*
Mulliken Center for Theoretical Chemistry, Clausius Institute of Physical and Theoretical Chemistry, University of Bonn
Beringstr. 4+6, 53115 Bonn (Germany)

[b] *Prof. Dr. S. P. Nolan*
Department of Chemistry and Centre for Sustainable Chemistry, Ghent University
Building S3, Krijsglaan 281, 9000 Ghent (Belgium)

[c] *Prof. Dr. O. Hollóczki*
Department of Physical Chemistry, Faculty of Science and Technology, University of Debrecen
Egyetem tér 1, 4032 Debrecen (Hungary)
E-mail: holloczki.oldamur@science.unideb.hu

Supporting information for this article is available on the WWW under https://doi.org/10.1002/chem.202203636

the presence of weak bases (e.g. K_2CO_3) under aerobic, and environmentally benign conditions. The metals, for which the applicability of this route has been demonstrated, cover all coinage and platinum metals, and therefore this pathway provides a sustainable synthetic access to the catalysts enabling a remarkable portion of modern synthetic methods.

Beyond the development in the synthetic procedures, efforts were also devoted to understanding the underlying mechanism that allows for the formation of NHC complexes from the imidazolium salts in the presence of the weak bases.[19,22,23] It is reasonable to assume that the deprotonation of the imidazolium cation to produce the superbase carbene[24–26] would not be feasible by a weak base to an extent that would result in any reasonable reaction rate for the complex formation. In this regard, the "weak base route" shows a striking resemblance to the organocatalytic activity of azolium salts,[27–32] in which carbene-like reactions can be observed with various substrates, with weak bases being present in the reaction mixture. The multiple contradictions and discrepancies in the mechanistic picture on these reactions[33] were resolved through suggesting a direct, concerted mechanism, in which the deprotonation of the azolium salt and the formation of the substrate-catalyst bond occur simultaneously, avoiding the formation of a free carbene in solution (Figure 2).[33–36] Analogous reaction mechanisms have been considered also for the biochemical reactions of thiamine,[36] the proton-deuteron exchange of azolium salts,[37,38] and the formation of azolium-2-dithiocarboxylate zwitterions.[39]

Tzouras et al. investigated the mechanism of the reaction between 1,3-bis(diisopro-pylphenyl)imidazolium chloride ([**IPrH**][Cl]) with [Au(SMe_2)Cl] in the presence of NEt_3 through computational chemical methods (Figure 3).[22] They found that the formation of an aurate intermediate [**IPrH**][$AuCl_2$] is exergonic. Although one can argue that the formation of the ion pair containing this complex anion may facilitate the deprotonation of the azolium cation, pK_a measurements indicated no anion effects on its acidity.[40] The aurate intermediate can, however, undergo a transformation in the presence of the weak amine base, which involves the cleavage of the C–H bond, and the simultaneous formation of the C–Au bond,[22] in a very similar mechanism to that of the organocatalytic reactions mentioned above (cf. Figure 2 and Figure 3). In the course of this rearrangement, a chloride anion dissociates from the metal, resulting in the desired complex and the [$HNEt_3$][Cl] salt. The barrier of this step was found to be affected by the deprotonation energy of the imidazolium precursor, as well as steric effects arising from the imidazolium cation and from the carbene. The stepwise mechanism – that involves the generation of the free carbene in the reaction mixture, and the subsequent association and reaction with the gold species – showed higher barriers, suggesting the dominance of the concerted, associative path.

Considering such an associative mechanism for the "weak base route" in general may eventually lead to an explanation of how the reaction can occur at all. However, there are curious experimental findings, which imply that the reaction is far from being understood. With the increasing basicity of the deprotonating agent, the theoretically calculated reaction barrier becomes lower in the associative mechanism of the organocatalytic reactions.[36] Although a similar effect could be expected for the complex formation as well, in case of these processes the experiments show, remarkably, somewhat contradictive trends. It has been observed that while K_2CO_3 can be applied as a base successfully for most of these reactions, using NEt_3 allows the formation of the targeted complexes only in a few cases.[19,22] However, using NaOAc as base in the reaction leads to lower energy barriers than NEt_3, despite its significantly lower pK_a in water.[23] Whereas this finding could be explained by the varying basicity of these compounds in different media, effects other than mere basicity may also be at play in these reactions, making the inorganic bases more competent.

The synthesis of metal-NHC complexes would benefit from understanding the fundamental principles that govern the underlying reactions, since it would enable identifying those factors in the processes, which can be further improved. Thus, in this contribution we aim at shedding light on hitherto

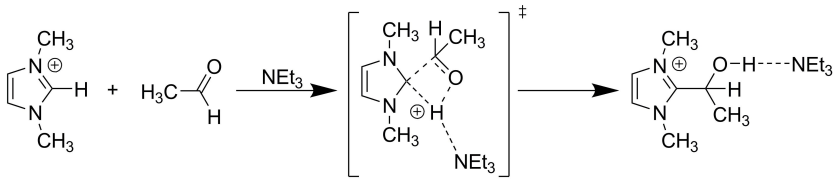

Figure 2. Alternative, concerted (associative) reaction mechanism discovered for NHC organocatalysis, avoiding the formation of a free carbene.[34,36]

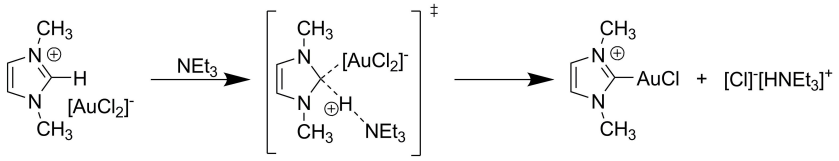

Figure 3. Reaction mechanism proposed for the weak base route by Tzouras et al., circumventing the formation of a free carbene.[22]

unknown aspects of the "weak base route", to reveal the effects that make one base more effective than the other in the corresponding synthetic approaches. To this end, we present here a detailed quantum chemical and molecular dynamics study on the reaction mechanism, and the solvent behavior within the reaction mixtures.

Results and Discussion

To investigate the effects of the reactants on the reaction mechanism, we chose 1,3-dimethylimidazolium chloride as a precursor, [*M*(DMS)Cl] (*M* = Au, Cu; DMS = dimethyl sulfide) as metal sources, and trimethylamine and sodium acetate as base. The overall four possible reactions were compared through high level DLPNO-CCSD(T)/CBS quantum chemical calculations, in terms of their reaction mechanism and energetics that may have an impact on the process. Based on earlier computational data,[22,34,36] we assumed that the reaction follows a concerted, associative pathway, in which the deprotonation of the imidazolium cation and the metal-carbon bond formation occur simultaneously.

The obtained reaction Gibbs free energy profiles are shown in Figures 4 and 5. The process is roughly similar in all four metal-base combinations. The first step is the association of the metal precursor and the 1,3-dimethylimidazolium chloride ion pair **I**, which forms the anionic dichloro complex of the metal **II**, releasing the dimethyl sulfide. Interestingly, this step – despite the high stability of the dichloro complexes – was found endergonic for gold in the solvent phase calculations. However, the subsequent evaporation of the sulfide would increase entropy, stabilizing **II** significantly. In **II**, the complex anion

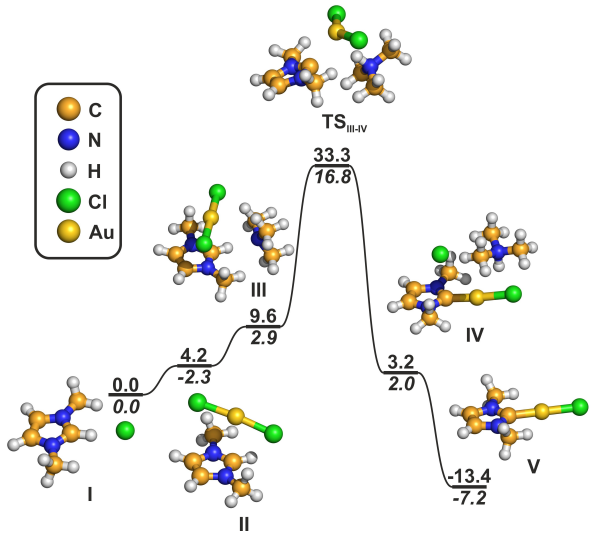

Figure 4. DLPNO-CCSD(T)/CBS Gibbs free energy profile (in kcal mol^{-1}) for the reaction of 1,3-dimethylimidazolium chloride with [*M*(DMS)Cl] (M = Au, above; M = Cu, below, italics) and trimethylamine, in acetone. Relative energies were calculated considering the presence of a fully dissociated [*M*(DMS)Cl] in the case of structure **I**, DMS in the case of structures **II**–**V**, and an [HN(CH$_3$)$_3$][Cl] ion pair in the case of structure **V**.

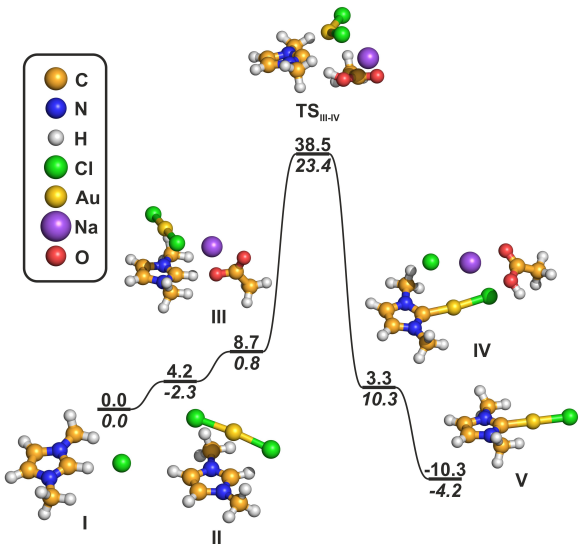

Figure 5. DLPNO-CCSD(T)/CBS Gibbs free energy profile (in kcal mol^{-1}) for the reaction of 1,3-dimethylimidazolium chloride with [*M*(DMS)Cl] (M = Au, above; M = Cu, below, italics) and sodium acetate, in acetone. Relative energies were calculated considering the presence of a fully dissociated [*M*(DMS)Cl] in the case of structure **I**, DMS in the case of structures **II**–**V**, and NaCl···HOAc in the case of structure **V**.

interacts with the imidazolium cation through its π-system. However, we localized another – albeit somewhat less stable – isomer of this structure (**IIa**, Figure 6), in which the gold and chlorine atoms form hydrogen bonds with the position 2 hydrogen atom of the ring (H2) and methyl hydrogen atoms. The small energy difference between these two structures suggests that they may be both present in the solution.

After forming the complex anion, the base and **II** associate into cluster **III**, which is – partly due to entropic effects – again endergonic. In **III**, the base forms a hydrogen bond with the imidazolium cation through the H2, while the anion is situated in a fashion that it can interact with the cationic π-system via van der Waals and Coulombic interactions. This cluster can be rearranged into structure **IIIa** (Figure 6), in which the complex anion occupies the site with a hydrogen bond to H2, whereas the base interacts with the π-system. However, according to the relative Gibbs free energies, **IIIa** is in all cases less stable than **III**.

After the formation of **III**, in which the base, the imidazolium cation, and the anionic metal source are associated, the complex formation can occur in a single elementary step, through **TS$_{III\rightarrow IV}$**. This step involves the proton transfer from the

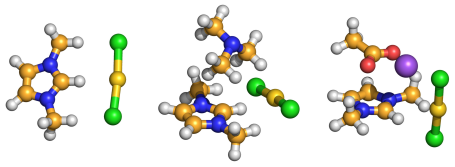

Figure 6. Ball-and-stick images of the isomers of **II** and **III**, structures **IIa** (left) and **IIIa** (with trimethylamine: center; with NaOAc: right).

imidazolium cation to the base, the formation of the *M*–C bond, and the cleavage of a *M*–Cl bond. This complicated rearrangement decreases the Gibbs free energy of the system and produces the desired metal-NHC complex. The dissociation of the protonated base in hydrogen bond with the chloride anion from the metal complex is also exergonic, resulting in an overall negative reaction Gibbs free energy, and thereby a driving force for the reaction. The transition states of all four reactions are collected in Figure 7. It is interesting to point out that in the $\mathbf{TS_{III\rightarrow IV}}$ structures found for the sodium acetate base, the strong and directional interaction between the sodium ion and the acetate anion hinders the arrival of the proton to the oxygen atom in a fashion that yields the usually most stable, *trans* conformation for the H–O–C–C dihedral angle, resulting in somewhat unexpected geometries.

The Gibbs free energy profiles exhibit remarkable differences between the four reactions. It is striking at first glance that the relative Gibbs free energies of the intermediates and the transition state of the reactions that involve copper are generally lower than those for the corresponding gold derivatives, indicating that the process can occur under milder conditions for the lighter transition metal. However, interestingly, the reaction is less exergonic for the copper derivatives. Exchanging the base has a milder, but still observable effect on the reaction. Generally, sodium acetate forms more stable complexes with **II**, showing that the ionic nature of the ion pair, that is, the corresponding high dipole moment makes it easier for the starting materials to associate. In contrast, the barriers of the reactions with the amine base are generally lower, suggesting that the amine produces the metal complex faster. As described above, this is in clear contradiction with the experimental findings, in which ionic bases show significantly higher reaction rates.[23]

To find where this conspicuous discrepancy between the quantum chemical results and the experimental findings from literature originates, it is worth looking at the factors these calculations fail to take into consideration. Since in the quantum chemical results the advantage of the ionic base is not apparent, it is also likely that finding the relevant shortcomings of this method will also reveal the source of the excellent performance for these bases.

First, the solubility of the two bases in solution is different. In the model taken above, a single amine molecule, or a sodium acetate ion pair reacts with the other reaction partners. Comparing these two reactions directly may not fully represent reality, since whereas the amine forms a homogeneous mixture with acetone, sodium acetate is a salt, and its saturated concentration in the organic solvent is significantly lower. This inherent difference between the two bases would, however, further decrease the potency of the acetate base, and the reaction rate. Second, the substituents on the imidazolium cation may influence the barriers through steric hindrance, changing the trends in the synthetically applied, realistic reaction mixtures. However, we found that the relative Gibbs free energy of $\mathbf{TS_{III\rightarrow IV}}$ with respect to **I** is barely altered when introducing the sizable 2,6-diisopropylphenyl (DIPP) substituents at the ring nitrogen atoms. At the B3LYP-D3BJ/def2-TZVPP level, this was found to be $\Delta G = 30.1$ kcal mol^{-1} (M = Au, R = DIPP), $\Delta G = 30.3$ kcal mol^{-1} (M = Au, R = Me), $\Delta G = 20.1$ kcal mol^{-1} (M = Cu, R = DIPP), and $\Delta G = 17.0$ kcal mol^{-1} (M = Cu, R = Me) with the trimethylamine base. Third, solution phase entropy calculations bear an error, which may affect the results even in a qualitative fashion and alter trends of reaction rates. This question has been under scrutiny from computational chemists for decades.[41–43] This error becomes significant, whenever there is a phase transfer in the reaction, if it involves a dissociation or association of particles. In this case, when comparing the Gibbs free energies for the two bases here, the association/dissociation processes are similar, therefore the error stemming from the faulty entropy estimation should also be similar, hence it should not break the trends. The fourth possibility is that there are complex liquid dynamics at play in these reactions, which have a severe influence on the rate of these reactions. Thus, among all conceivable reasons mentioned above, only the latter seems likely, hence we decided to investigate this issue in more detail.

It is clear from the literature that ionic bases exhibit the higher potency in aiding the reaction at hand, and thus this feature deserves a special focus when discussing the structure and dynamics of the reaction mixture. Ionic compounds have a particular behavior in solution, which can be characterized by the association or dissociation of the counterions. In weak electrolytes, the anions and cations are dissociated only to a small extent, forming ion pairs or larger aggregates in solution, whilst in strong electrolytes the counterions fully separate, and move independently. This feature is of key importance in electrochemical applications, but it can have severe consequences on reactivity as well (e.g. in controlling the mechanism of S_N reactions).[44–47]

Ion pairing has been investigated extensively for ionic liquids.[48,49] These compounds[50–53] are generally composed of organic cations (often 1,3-dialkylimidazolium derivatives), and

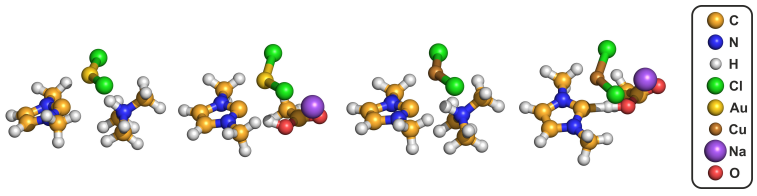

Figure 7. Ball-and-stick images of the transition states $\mathbf{TS_{III\rightarrow IV}}$ of the metal-NHC complex formation reactions of the 1,3-dimethylimidazolium cation found by quantum chemical calculations.

inorganic anions (e.g. halides, main group halide complexes, carboxylates),[54] which make them very similar to the precursors that are involved in the "weak base route". Remarkably, ionic liquids in molecular solvents form ion pairs or aggregates in many cases.[55–59] In relation to the organocatalytic activity of azolium cations, the dissociation free energy of ion pairs of various 1,3-dimethylimidazolium salts have been investigated in a range of organic solvents and water through classical molecular dynamics simulations.[36] The formation of ion pairs was favorable in most cases, only the 1,3-dimethylimidazolium chloride showed some tendency to dissociate in water, probably due to the high solvation energy of the anion in this highly polar solvent.

Based on these data it is reasonable to assume that the reactivity of the imidazolium salt, and the association of the base with the acidic hydrogen atom of the imidazolium cation are strongly influenced by these strong, long-range ion-ion interactions. Since the reaction requires the simultaneous aggregation of the imidazolium cation, the metal complex anion, and the base in a manner where the base can also access the acidic hydrogen of the cation, the effects that influence association processes in solution may be decisive for the reaction. To test these hypotheses, classical molecular dynamics simulations were performed. For the high-end quantum chemical calculations described above, the small methyl groups were chosen to rationalize computational demand, and since steric effects seem to have a very low impact on the reaction mechanism and energetics in similar reactions.[36] This was also corroborated by DFT calculations comparing the 2,6-diisopropylphenyl and methyl substituted imidazolium derivatives (see data and discussion above). For the classical molecular dynamics simulations, however, computational time is not an issue, and the solvent dynamics at the imidazolium ring should be highly affected by the size of the substituents on the nitrogen atoms.[38,60] Thus, for these models we took the structure that was most often investigated in experimental mechanistic studies, 1,3-bis(2,6-diisopropylphenyl)imidazolium (**IPr**).[61] Aiming at revealing the structural and dynamic details of ion pairing, and its effects on the reaction, we created two sets of models. In the first set, a single ion pair of [**IPrH**]$^+$ with a variety of anions [X]$^-$ (chloride [Cl]$^-$, tetraphenyloborate [BPh_4]$^-$, bis(trifluoromethanesulfonyl)imide [NTf_2]$^-$, acetate [OAc]$^-$, [$AuCl_2$]$^-$) was modeled in a series of solvents with different polarity and hydrogen bonding ability (acetone, methanol, glycol, 1,1,1,3,3,3-hexafluoropropan-2-ol HFIP, 1-butylpyridinium tetrafluoroborate [BuPy][BF_4]). For these systems the dissociation free energy was calculated through umbrella integration. In the second set of simulations, ten ion pairs [**IPrH**][X] and ten base molecules (of either triethylamine, or sodium acetate) were dissolved in various solvents and with various kinds of [X]$^-$, to observe association processes in a realistic reaction mixture, and the preference for the base to interact with the acidic proton. The composition of the systems is shown in the Supporting Information.

The [**IPrH**][Cl] ion pair exhibited a wide range of behavior in different solvents (Figure 8), and the calculations also indicated very different dissociation energies as well (Table 1).

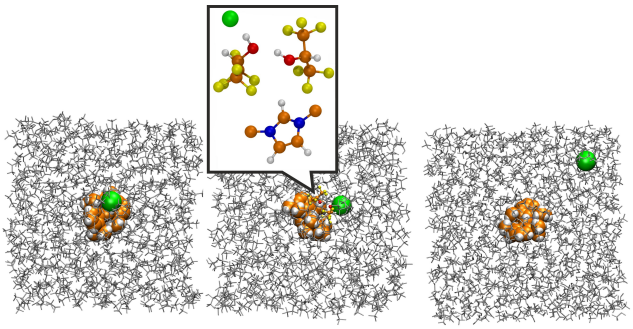

Figure 8. Representative snapshots of the molecular dynamics simulations with 1,3-bis(2,6-diisopropylphenyl)imidazolium chloride in acetone (left), 1,1,1,3,3,3-hexafluoropropan-2-ol (middle), and methanol (right).

Table 1. Dissociation free energies (in kcal mol^{-1}) for the [**IPrH**][X] ion pair in various solvents ([BuPy][BF_4]: 1-butylpyridinium tetrafluoroborate; [BPh_4]$^-$: tetraphenyloborate anion; [NTf_2]$^-$: bis(trifluoromethanesulfonyl)imide anion; HFIP: 1,1,1,3,3,3-hexafluoropropan-2-ol).

X	[OAc]$^-$	[Cl]$^-$	[NTf_2]$^-$	[BPh_4]$^-$	[$AuCl_2$]$^-$
acetone	1.8	3.9	0.1	−2.3	−0.1
methanol	−2.5	−3.1	0.0	0.1	−0.2
glycol	−3.0	−8.0	1.2	−1.1	3.8
HFIP	9.8	10.9	10.4	−3.0	7.1
[BuPy][BF_4]	0.8	−3.8	3.9	12.7	−3.0

In acetone – the solvent of choice in most of the corresponding applications – the ion pair stayed intact, requiring 3.9 kcal mol^{-1} free energy for the dissociation, indicating strong ion pairing. Introducing hydrogen bond donor sites into the solvent improves the solvation of the anion, which facilitates dissociation. Thus, in methanol and glycol the [**IPrH**][Cl] ion pair dissociates into free ions due to the −3.1 and −8.0 kcal mol^{-1} dissociation free energies, respectively. Interestingly, the strong hydrogen bond donor 1,1,1,3,3,3-hexafluoropropan-2-ol (HFIP) does not aid dissociation, and produces a 10.9 kcal mol^{-1} dissociation free energy for the [**IPrH**][Cl] ion pair. This finding can be rationalized by the large fluorous groups of the solvent, which form a microheterogeneous structure[62–64] with large non-polar domains that are dominated by the negatively polarized fluorous groups. Instead, in the simulations HFIP exhibited an interesting behavior, inserting one or two -OH groups between the H2 of the [**IPrH**]$^+$ cation and the chloride anion, inducing the formation of a solvent separated ion pair (Figure 8 middle). In the dissociation free energy calculations, for the structures with the H2-Cl distances that correspond to the solvent separated ion pair, a relative energy of −1.5 kcal mol^{-1} was found. In the ionic liquid 1-butylpyridinium tetrafluoroborate ([BuPy][BF_4]), full dissociation of [**IPrH**][Cl], and a dissociation energy of −3.8 kcal mol^{-1} was observed. This is reasonable as ionic liquids have been known to be "superdissociative" solvents, inducing the formation of free ions from ionic solutes.[46,47]

Ion pairing depends on the strength of the cation-anion interaction, and its relation to the cation-solvent and anion-solvent interplay,[44,65] as well as the size disparity of the ions

and the solvent.[66] If the charge of the ions is more delocalized, the directionality of the cation-anion interaction is decreased, and it becomes weaker. Exchanging the chloride anion to an $[NTf_2]^-$ decreases the dissociation energy of the ion pair in acetone to 0.1 kcal mol^{-1}. Since the $[NTf_2]^-$ anion is a weaker hydrogen bond acceptor than chloride, hydrogen bond donor solvents are expected to stabilize the free anion less than in case of the halide. In agreement, the dissociation free energies did not decrease in HFIP upon introducing this anion, while in methanol, glycol and [BuPy][BF_4] a notable decrease can be observed. Interestingly, for HFIP again the formation of a solvent separated ion pair was observed, which was found −1.0 kcal mol^{-1} lower in free energy than the ion pair. In case of the even larger $[BPh_4]^-$ anion, dissociation free energy decreases further in acetone, and dissociation becomes spontaneous. Due to the lack of hydrogen bonding sites, [**IPrH**][BPh_4] ion pairs exhibit higher dissociation free energies in methanol and glycol than the corresponding chlorides. However, interestingly, dissociation becomes thermodynamically favorable in HFIP, whilst increasing in the ionic liquid. Thus, it is apparent that while in acetone and HFIP the increasing size and charge delocalization on the anion is advantageous for separating the cation and the anion, in the ionic liquid it is disadvantageous, as it results in a decrease in solute-solvent ion-ion interactions, and thereby the driving force for dissociation is diminished.

From a practical point of view, the acetate and dichloroaurate ions are the most relevant in the present selection, as they represent a possible base and metal source in the metal-NHC complex formation processes. The acetate anion is the base that should remove the proton from the ring, as the dichloroaurate loses a chloride anion and forms a gold-carbon bond. The separation of the acetate anion from the imidazolium ring is endothermic in acetone, but the free energy difference is lower than what one could expect from a basic, strong hydrogen bond acceptor anion. In methanol and glycol the separation becomes exothermic, showing that the hydrogen bonding from the solvent molecules can split the ion pair. Interestingly, despite these obvious effects, HFIP hinders the dissociation, in which probably the fluorous groups play a key role. Separation of the anion and cation in the ionic liquid solvent has a low energy demand.

In case of the gold complex, interestingly, the dissociation from the imidazolium cation is energetically neutral in acetone and methanol. However, in both solvents, upon increasing the distance between the acetate and the H2 of [**IPrH**]$^+$, lower energy structures were formed, in which the metal complex anion was situated at the 4 and 5 position atoms of the ring. The free energy of this state was found 0.8 and 0.6 kcal mol^{-1} lower than that of the dissociated system for acetone and methanol, respectively. While in HFIP and glycol the ion pair is apparently stable, in the ionic liquid it tends to dissociate.

In the second set of simulations, the close approach of the base to the acidic hydrogen of the imidazolium cation can be observed directly (Table 2). In the probabilities of the close [**IPrH**]$^+$-base contacts (H–O or H–N distance smaller than 3 Å), several trends can be observed. For the [**IPrH**][Cl] salt, the NEt_3 shows an observable, but low peak at the hydrogen bonding distance. Interestingly, in methanol this peak increases, while in glycol and HFIP it fully disappears. In the ionic liquid [BuPy][BF_4], however, the amine and the imidazolium cation are again prone to association, showing a distinct high peak. These results can be rationalized through the ion pairing that keeps the chloride anion at the H2 in acetone. In methanol the hydrogen bonding between the chloride and the solvent dissociates the [**IPrH**][Cl], and thereby liberates the H2 for interaction with the amines, but the hydrogen bonding with the cation must compete with the methanol-amine interplay, hence the peak becomes only slightly higher. Increasing hydrogen bond donor character of the solvent shifts this competition, resulting in no measurable peaks for glycol and HFIP. In case of HFIP, this effect is emphasized even more due to the importance of the solvent separated ion pair structure, which blocks the cation-base interaction. With its sizable diisopropylphenyl groups, [**IPrH**]$^+$ is larger than [BuPy]$^+$ and has more non-polar groups as well. Thus, its association with the amine may be facilitated not only by the strength of the C–H···N hydrogen bond, but also by hydrophobic interactions. These are also not hindered by the presence of the chloride, as a full dissociation of this ion pair occurs in this system (Table 1).

In hydrogen bonding solvents, sodium acetate has contacts less often with the imidazolium cation, than in acetone, as the acetate anion forms interactions rather with these solvent molecules, instead of the reactant. NEt_3 seems to be less sensitive to this effect, being a significantly weaker hydrogen bond acceptor. The ionic liquid [BuPy][BF_4] has a generally low performance as a solvent, as it appears to be hindering the imidazolium/base contacts effectively, except for [**IPrH**][Cl].

Table 2. Peak heights for the first peaks in the H···O/N radial pair correlation functions, describing the probability of a hydrogen bond formation between the H2 in [**IPrH**]$^+$, and the oxygen (NaOAc) or nitrogen (NEt_3) atom of the base.

X	B	acetone	methanol	glycol	HFIP	[BuPy][BF_4]
$[Cl]^-$	NEt_3	0.20	0.47	0.00	0.00	2.89
$[NTf_2]^-$	NEt_3	0.41	0.42	1.68	0.51	0.00
$[BPh_4]^-$	NEt_3	0.42	0.40	0.08	0.06	0.00
$[AuCl_2]^-$	NEt_3	0.35	0.28	0.27	1.00	0.00
$[Cl]^-$	NaOAc	7.77	0.26	0.07	0.04	0.00
$[NTf_2]^-$	NaOAc	1.98	0.02	0.01	0.13	0.00
$[BPh_4]^-$	NaOAc	1.40	0.06	0.09	0.01	0.00
$[AuCl_2]^-$	NaOAc	4.83	0.13	0.01	0.00	0.00

The lower propensity of [**IPrH**][NTf_2] and [**IPrH**][BPh_4] to form ion pairs in acetone results in two times higher peaks in the radial pair correlation functions (RDFs) than the chloride salt in the same solvent in case of the amine base. On the other hand, since ion pairing in [BuPy][BF_4] occurs significantly more often with these two anions than with the chloride (Table 1), in this ionic liquid the H2 is blocked from the NEt_3. In methanol, the $g(r)$ values slightly decrease with respect to the chloride analogue. For the $[BPh_4]^-$ derivative, the imidazolium-amine interaction has a low occurrence, again similarly to the chloride. Interestingly, however, HFIP and especially glycol exhibit significant RDF peaks for the [**IPrH**]$^+$-NEt_3 interaction.

Regarding the experiments, the $[AuCl_2]^-$ anion is the most relevant. The [**IPrH**][$AuCl_2$] ion pair can occasionally interact with the amine base through the H2 in all solvents, except for the ionic liquid. Interestingly, HFIP allows for the by far most frequent [**IPrH**]$^+$-NEt_3 interplay, making it a solvent of interest for the reactions, if for some reason an amine base must be employed.

In acetone, the acetate base shows already at first glance much higher $g(r)$ values than NEt_3 (Table 2), all values being above 1. This is especially the case for the chloride salt, which exhibits a prominent $g(r) = 7.77$, followed closely by the $[AuCl_2]^-$ with a $g(r) = 4.83$. In the latter case, with the [**IPrH**][$AuCl_2$] and the base in the solution, the association represented in Table 2 can directly be rationalized as the formation of cluster **III** (Figures 4 and 5). These results can be explained through the strong ion pairing behavior, which aids the association of these two species (Table 1). It is also remarkable, that the chloride anion has a very strong interaction with the [**IPrH**]$^+$, outperforming all other anions in the non-hydrogen bonding solvent acetone. In the rest of the solvents the base has significantly less access to the H2, which is in line with the lower dissociation energies presented in Table 1. Thus, due to their hydrogen bond acceptor properties, methanol, glycol, HFIP and the ionic liquid [BuPy][BF_4] form strong interactions with the acetate anion, efficiently competing for this base with the [**IPrH**]$^+$. To observe if steric effects play a role in the association processes in question, we performed simulations for 1,3-dimethylimidazolium dichloroaurate in acetone with the two bases, in a setup identical to those presented in Table 2. The corresponding first peak heights exhibited a very similar trend compared to the system with the sizable 2,6-diisopropylphenyl substituted compounds, with $g(r) = 0.48$ for NEt_3, and $g(r) = 17.13$ for NaOAc.

As mentioned above, the combination of the solvent acetone with the base sodium acetate produced the best results in the experimental setup from all the systems that we have investigated theoretically here. The acetate base is outperformed only by carbonates, which are on one hand also ionic substances, and stronger bases. It is remarkable, that the classical molecular dynamics simulations reproduced the prominence of the above solvent/base combination, which indicates that the observed underlying effects are decisive, or at least play a significant role in determining the rate of metal-NHC complex formation via the "weak base route".

The mechanistic picture above has implications also beyond the "weak base route". In case of the "built-in base route", the base that facilitates the process is inherently associated with the other components, either as a ligand at the metal source, or the counterion of the imidazolium precursor. Thus, in these roles, the base can be more active, and the reaction rate can be higher.

Conclusion

The "weak base route" has emerged in the literature as the most efficient way to synthesize metal-*N*-heterocyclic carbene complexes. The key to this method is the application of a weak base that does not promote the formation of a free carbene in the solution, thus making the reaction mixture easier to handle. These bases should be, on the other hand, able to abstract a proton from the precursor imidazolium cation, while it is reacting with the metal source. Earlier experimental evidence indicates that the basicity of the base is not the only decisive factor in the efficiency of the reaction. While in aqueous solutions acetates have a lower basicity than amines, the latter compounds fail to promote complex formation, and the former ones show a high activity.

We show that the reason for this difference does not lie in the reactivity *per se*, but in the ability of the base to access the proton it is to remove. Whereas the amine base is kept away from this site by the counterion of the imidazolium cation, ionic bases can efficiently compete for the proton in question. The tendency of ionic compounds to associate in solution brings all the components of the reaction, the imidazolium cation, base, and metal source, into a cluster, in which the reaction can occur, thereby facilitating complex formation. Thus, it is apparent that these effects explain why not all weak bases are amenable in these reactions and *that the ability of* the aforementioned driving forces to enhance the association with the imidazolium precursor should be considered, when selecting the appropriate components for the reaction.

Computational Methods

Quantum Chemical Calculations

Quantum chemical calculations were performed by the Orca program version 4.2.1.[67] All structures were fully optimized using the B3LYP functional,[68,69] augmented with the D3 dispersion correction with Becke–Johnson damping,[70,71] together with the def2-TZVPP basis set.[72,73] For both the geometry optimization and the SCF cycle tight convergence criteria were set. The nature of the obtained stationary points was confirmed by having no negative eigenvalues of the Hessian in case of minima, and exactly one negative eigenvalue for transition states. For each transition state, a steepest descent geometry optimization was performed in both directions defined by the imaginary normal mode to identify the minima connected by the given transition state. On the optimized structures, DLPNO-CCSD(T)/CBS calculations were performed in an extrapolation scheme based on the def2-TZVPP and def2-QZVPP single point energies, with tight settings on the localization.[74–77]

The total Gibbs free energy of the structures was obtained as the sum of the DLPNO-CCSD(T)/CBS electronic energies, the B3LYP-D3BJ/def2-TZVPP thermal corrections, and the solvation Gibbs free energies from B3LYP-D3BJ/def2-TZVPP single point calculations using the CPCM implicit solvation model for acetone as solvent.[78]

The protocol that was used to calculate the *Gibbs* free energies for each structure:

- perform B3LYP-D3BJ/def2-TZVPP optimization and frequency calculation to obtain structures and $(G–E)_{B3LYP}$
- perform B3LYP-D3BJ/def2-TZVPP/CPCM(acetone) single point calculations to obtain ($E_{B3LYP,solv}$) and additionally:
- CPCM electrostatic contribution (E_{ENP})
- CPCM cavity dispersion correction (E_{CDS})
- perform DLPNO-CCSD(T)/def2-TZVPP single point calculations ($E_{CCSD(T)/TZ}$)
- perform DLPNO-CCSD(T)/def2-QZVPP single point calculations ($E_{CCSD(T)/QZ}$)
- extrapolate SCF- and correlation energies obtained from CCSD(T) calculations to the complete basis set ($E_{CCSD(T)/CBS}$)
- add E_{ENP} and E_{CDS} to CCSD(T) total energies to in order to include solvation effects and obtain $E_{CCSD(T)/TZ,solv}$, $E_{CCSD(T)/QZ,solv}$ and $E_{CCSD(T)/CBS,solv}$
- to obtain *Gibbs* free energies (G): add the thermodynamic contribution $(G–E)_{B3LYP}$ to the electronic energies (with solvation effects)

Molecular Dynamics Simulations

Molecular dynamics simulations were performed with the Lammps program package.[79] For the organic solvents, sodium acetate, triethylamine and the 1,3-diisopropylphenyl substituents the standard OPLS-AA parameters were applied,[80] while for 1,1,1,3,3,3-hexafluoroisopropan-2-ol (HFIP) the force field reported by Fioroni et al. was used.[81] Given the similarity of the hereby investigated imidazolium salts and ionic liquids, for the imidazolium moiety the force field parameters of Pádua and Canongia Lopes were used, exploiting their compatibility with the OPLS-AA model.[54,82,83] The 1-butylpyridinium tetrafluoroborate solvent was modeled by the same force fields for ionic liquids.[83] For the tetraphenyloborate anion, the standard OPLS Lennard-Jones parameters, and the charges reported by Schurhammer and Wipff were employed.[84]

The simulation boxes for producing the data in Table 1 were composed of a single ion pair of [IPrH][X] each, and 500 acetone, 1000 methanol, 750 glycol, 400 HFIP, or 300 [BuPy][BF_4] ion pairs. The second set of simulations, used for the data in Table 2, were composed of 10 [IPrH][X] ion pairs, 10 bases (NEt_3 or NaOAc), and 1000 acetone, 2000 methanol, 1500 glycol, 750 HFIP, or 500 [BuPy][BF_4] ion pairs. The simulation boxes were created with the Packmol program package.[85] After an initial energy minimization, the system was simulated in an NpT ensemble using Nosé–Hoover thermostats (T = 320 K, with a time constant of 100 fs) and barostats (p = 1 bar, with a time constant of 2 ps) for 7 ns. For the last 6 ns the box volume was averaged and used to calculate the cell vectors to be used for the subsequent simulations. After 1.5 ns of further equilibration in the NVT ensemble, an NVT production run was performed for 20 ns. The analysis of the systems was performed by using the Travis program.[86,87]

In case of the umbrella integration calculations, an external harmonic potential was added to the system produced by the protocol above, which kept the distance between the H2 atom of the imidazolium ring and the central atom of the anion short (Cl for chloride, B for $[BPh_4]^-$, N for $[NTf_2]^-$; carboxylate C for $[OAc]^-$; Au for $[AuCl_2]^-$, at e.g. 2.25 Å for chloride). After 1 ns of equilibration, the force that acted on the above potential was measured and averaged over a production run of 250 ps. The selected interatomic distance was then increased by increments of 0.25 Å until 20 Å, repeating the equilibration and production runs at each distance. Integrating the forces versus the distance gave the free energy profile of the ion pair separation.

Acknowledgements

J.B. acknowledges financial support by the Deutsche Forschungsgemeinschaft (DFG) through the grant project number 406232243. For work carried out in Ghent, S.P.N. is grateful to the FWO and the BOF (starting and senior grants) as well as to the iBOF C3 project for financial support. The financial support for O.H. by the National Research, Development and Innovation Office through the project OTKA-FK 138823 is gratefully acknowledged. Furthermore, O.H. is grateful for the support from the János Bolyai Research Scholarship of the Hungarian Academy of Sciences, and the ÚNKP-22-5 New National Excellence Program from the National Research, Development and Innovation Fund.

Conflict of Interest

The authors declare no conflict of interest.

Data Availability Statement

The data that support the findings of this study are available in the supplementary material of this article.

Keywords: basicity · carbene complexes · *N*-heterocyclic carbenes · reaction mechanisms

[1] S. Díez-González, N. Marion, S. P. Nolan, *Chem. Rev.* **2009**, *109*, 3612–3676.
[2] S. P. Nolan, *Acc. Chem. Res.* **2011**, *44*, 91–100.
[3] Q. Zhao, G. Meng, S. P. Nolan, M. Szostak, *Chem. Rev.* **2020**, *120*, 1981–2048.
[4] K. H. Doetz, J. Stendel Jr, *Chem. Rev.* **2009**, *109*, 3227–3274.
[5] A. Chartoire, C. Claver, M. Corpet, J. Krinsky, J. Mayen, D. Nelson, S. P. Nolan, I. Peñafiel, R. Woodward, R. E. Meadows, *Org. Process Res. Dev.* **2016**, *20*, 551–557.
[6] P. de Frémont, N. M. Scott, E. D. Stevens, S. P. Nolan, *Organometallics* **2005**, *24*, 2411–2418.
[7] N. P. Mankad, T. G. Gray, D. S. Laitar, J. P. Sadighi, *Organometallics* **2004**, *23*, 1191–1193.
[8] N. Schneider, V. César, S. Bellemin-Laponnaz, L. H. Gade, *J. Organomet. Chem.* **2005**, *690*, 5556–5561.
[9] M. S. Viciu, O. Navarro, R. F. Germaneau, R. A. Kelly, W. Sommer, N. Marion, E. D. Stevens, L. Cavallo, S. P. Nolan, *Organometallics* **2004**, *23*, 1629–1635.
[10] M. R. Furst, C. S. Cazin, *Chem. Commun.* **2010**, *46*, 6924–6925.
[11] I. J. Lin, C. S. Vasam, *Coord. Chem. Rev.* **2007**, *251*, 642–670.
[12] C. A. Citadelle, E. Le Nouy, F. Bisaro, A. M. Slawin, C. S. Cazin, *Dalton Trans.* **2010**, *39*, 4489–4491.
[13] R. A. Kelly, N. M. Scott, S. Díez-González, E. D. Stevens, S. P. Nolan, *Organometallics* **2005**, *24*, 3442–3447.
[14] N. Marion, E. C. Ecarnot, O. Navarro, D. Amoroso, A. Bell, S. P. Nolan, *J. Org. Chem.* **2006**, *71*, 3816–3821.

[15] H. Rodríguez, G. Gurau, J. D. Holbrey, R. D. Rogers, *Chem. Commun.* **2011**, *47*, 3222–3224.
[16] O. Hollóczki, *Inorg. Chem.* **2013**, *53*, 835–846.
[17] S. Wellens, N. R. Brooks, B. Thijs, L. Van Meervelt, K. Binnemans, *Dalton Trans.* **2014**, *43*, 3443–3452.
[18] M. Fevre, J. Pinaud, A. Leteneur, Y. Gnanou, J. Vignolle, D. Taton, K. Miqueu, J.-M. Sotiropoulos, *J. Am. Chem. Soc.* **2012**, *134*, 6776–6784.
[19] E. A. Martynova, N. V. Tzouras, G. Pisanò, C. S. Cazin, S. P. Nolan, *Chem. Commun.* **2021**, *57*, 3836–3856.
[20] A. Collado, A. Gómez-Suárez, A. R. Martin, A. M. Slawin, S. P. Nolan, *Chem. Commun.* **2013**, *49*, 5541–5543.
[21] R. Visbal, A. Laguna, M. C. Gimeno, *Chem. Commun.* **2013**, *49*, 5642–5644.
[22] N. Tzouras, F. Nahra, L. Falivene, L. Cavallo, M. Saab, K. Van Hecke, A. Collado, C. J. Collett, A. D. Smith, C. Cazin, S. P. Nolan, *Chem. Eur. J.* **2020**, *26*, 4515–4519.
[23] T. Scattolin, N. V. Tzouras, L. Falivene, L. Cavallo, S. P. Nolan, *Dalton Trans.* **2020**, *49*, 9694–9700.
[24] Y.-J. Kim, A. Streitwieser, *J. Am. Chem. Soc.* **2002**, *124*, 5757–5761.
[25] R. W. Alder, P. R. Allen, S. J. Williams, *J. Chem. Soc. Chem. Commun.* **1995**, 1267–1268.
[26] T. L. Amyes, S. T. Diver, J. P. Richard, F. M. Rivas, K. Toth, *J. Am. Chem. Soc.* **2004**, *126*, 4366–4374.
[27] D. Enders, O. Niemeier, A. Henseler, *Chem. Rev.* **2007**, *107*, 5606–5655.
[28] N. Marion, S. Díez-González, S. P. Nolan, *Angew. Chem. Int. Ed.* **2007**, *46*, 2988–3000; *Angew. Chem.* **2007**, *119*, 3046–3058.
[29] D. Enders, T. Balensiefer, *Acc. Chem. Res.* **2004**, *37*, 534–541.
[30] M. N. Hopkinson, C. Richter, M. Schedler, F. Glorius, *Nature* **2014**, *510*, 485–496.
[31] X. Bugaut, F. Glorius, *Chem. Soc. Rev.* **2012**, *41*, 3511–3522.
[32] D. M. Flanigan, F. Romanov-Michailidis, N. A. White, T. Rovis, *Chem. Rev.* **2015**, *115*, 9307–9387.
[33] O. Hollóczki, *Chem. Eur. J.* **2020**, *26*, 4885.
[34] S. Gehrke, O. Hollóczki, *Angew. Chem. Int. Ed.* **2017**, *56*, 16395–16398; *Angew. Chem.* **2017**, *129*, 16613–16617.
[35] S. Gehrke, W. Reckien, I. Palazzo, T. Welton, O. Hollóczki, *Eur. J. Org. Chem.* **2019**, *2019*, 504–511.
[36] S. Gehrke, O. Hollóczki, *Chem. Eur. J.* **2020**, *26*, 10140.
[37] D. Rico del Cerro, R. Mera-Adasme, A. W. King, J. E. Perea-Buceta, S. Heikkinen, T. Hase, D. Sundholm, K. Wähälä, *Angew. Chem. Int. Ed.* **2018**, *57*, 11613–11617; *Angew. Chem.* **2018**, *130*, 11787–11791.
[38] O. Hollóczki, *Phys. Chem. Chem. Phys.* **2016**, *18*, 126–140.
[39] F. Mazars, M. Hrubaru, N. Tumanov, J. Wouters, L. Delaude, *Eur. J. Org. Chem.* **2021**, *2021*, 2025–2033.
[40] R. S. Massey, C. J. Collett, A. G. Lindsay, A. D. Smith, A. C. O'Donoghue, *J. Am. Chem. Soc.* **2012**, *134*, 20421–20432.
[41] S. Tobisch, T. Ziegler, *J. Am. Chem. Soc.* **2004**, *126*, 9059–9071.
[42] D. H. Wertz, *J. Am. Chem. Soc.* **1980**, *102*, 5316–5322.
[43] Y. B. Yu, P. L. Privalov, R. S. Hodges, *Biophys. J.* **2001**, *81*, 1632–1642.
[44] Y. Marcus, G. Hefter, *Chem. Rev.* **2006**, *106*, 4585–4621.
[45] M. John, C. Auel, C. Behrens, M. Marsch, K. Harms, F. Bosold, R. M. Gschwind, P. R. Rajamohanan, G. Boche, *Chem. Eur. J.* **2000**, *6*, 3060–3068.
[46] J. P. Hallett, C. L. Liotta, G. Ranieri, T. Welton, *J. Org. Chem.* **2009**, *74*, 1864–1868.
[47] M. Y. Lui, L. Crowhurst, J. P. Hallett, P. A. Hunt, H. Niedermeyer, T. Welton, *Chem. Sci.* **2011**, *2*, 1491–1496.
[48] B. Kirchner, F. Malberg, D. S. Firaha, O. Hollóczki, *J. Phys. Condens. Matter* **2015**, *27*, 463002.
[49] J. Ingenmey, O. Hollóczki, B. Kirchner, *Journal: Encyclopedia of Ionic Liquids* **2020**, 1–14.
[50] T. Welton, *Chem. Rev.* **1999**, *99*, 2071–2084.
[51] J. F. Brennecke, R. D. Rogers, K. R. Seddon, *Ionic Liquids IV. Not Just Solvents Anymore*, American Chemical Society, Washington, **2007**.
[52] R. D. Rogers, K. R. Seddon, *Science* **2003**, *302*, 792–793.
[53] T. Welton, *Green Chem.* **2011**, *13*, 225–225.
[54] B. Kirchner, O. Hollóczki, J. N. Canongia Lopes, A. A. Pádua, *WIREs Comput. Mol. Sci.* **2015**, *5*, 202–214.
[55] T. Singh, A. Kumar, *J. Phys. Chem. B* **2007**, *111*, 7843–7851.
[56] C. Spickermann, J. Thar, S. Lehmann, S. Zahn, J. Hunger, R. Buchner, P. Hunt, T. Welton, B. Kirchner, *J. Chem. Phys.* **2008**, *129*, 104505.
[57] M. Bešter-Rogač, M. V. Fedotova, S. E. Kruchinin, M. Klähn, *Phys. Chem. Chem. Phys.* **2016**, *18*, 28594–28605.
[58] M. Bešter-Rogač, A. Stoppa, R. Buchner, *J. Phys. Chem. B* **2014**, *118*, 1426–1435.
[59] J.-C. Jiang, K.-H. Lin, S.-C. Li, P.-M. Shih, K.-C. Hung, S. H. Lin, H.-C. Chang, *J. Chem. Phys.* **2011**, *134*, 044506.
[60] S. Gehrke, O. Hollóczki, *Chem. Eur. J.* **2018**, *24*, 11594–11604.
[61] J. Huang, S. P. Nolan, *J. Am. Chem. Soc.* **1999**, *121*, 9889–9890.
[62] M. Fioroni, K. Burger, A. E. Mark, D. Roccatano, *J. Phys. Chem. B* **2001**, *105*, 10967–10975.
[63] K. Yoshida, T. Yamaguchi, T. Adachi, T. Otomo, D. Matsuo, T. Takamuku, N. Nishi, *J. Chem. Phys.* **2003**, *119*, 6132–6142.
[64] O. Hollóczki, A. Berkessel, J. Mars, M. Mezger, A. Wiebe, S. R. Waldvogel, B. Kirchner, *ACS Catal.* **2017**, *7*, 1846–1852.
[65] O. Hollóczki, F. Malberg, T. Welton, B. Kirchner, *Phys. Chem. Chem. Phys.* **2014**, *16*, 16880–16890.
[66] H. Spohr, G. Patey, *J. Chem. Phys.* **2008**, *129*, 064517.
[67] F. Neese, *WIREs Comput. Mol. Sci.* **2012**, *2*, 73–78.
[68] A. D. Becke, *J. Chem. Phys.* **1993**, *98*, 5648–5652.
[69] C. Lee, W. Yang, R. G. Parr, *Phys. Rev. B* **1988**, *37*, 785.
[70] S. Grimme, J. Antony, S. Ehrlich, H. Krieg, *J. Chem. Phys.* **2010**, *132*, 154104.
[71] S. Grimme, S. Ehrlich, L. Goerigk, *J. Comput. Chem.* **2011**, *32*, 1456–1465.
[72] A. Schäfer, H. Horn, R. Ahlrichs, *J. Chem. Phys.* **1992**, *97*, 2571–2577.
[73] F. Weigend, R. Ahlrichs, *Phys. Chem. Chem. Phys.* **2005**, *7*, 3297–3305.
[74] C. Riplinger, B. Sandhoefer, A. Hansen, F. Neese, *J. Chem. Phys.* **2013**, *139*, 134101.
[75] D. G. Liakos, F. Neese, *J. Chem. Theory Comput.* **2015**, *11*, 4054–4063.
[76] D. G. Liakos, M. Sparta, M. K. Kesharwani, J. M. Martin, F. Neese, *J. Chem. Theory Comput.* **2015**, *11*, 1525–1539.
[77] D. G. Liakos, F. Neese, *J. Phys. Chem. A* **2012**, *116*, 4801–4816.
[78] V. Barone, M. Cossi, *J. Phys. Chem. A* **1998**, *102*, 1995–2001.
[79] S. Plimpton, *J. Comput. Phys.* **1995**, *117*, 1–19.
[80] W. L. Jorgensen, D. S. Maxwell, J. Tirado-Rives, *J. Am. Chem. Soc.* **1996**, *118*, 11225–11236.
[81] M. Fioroni, K. Burger, A. E. Mark, D. Roccatano, *J. Phys. Chem. B* **2001**, *105*, 10967–10975.
[82] J. N. Canongia Lopes, J. Deschamps, A. A. Pádua, *J. Phys. Chem. B* **2004**, *108*, 2038–2047.
[83] J. N. Canongia Lopes, A. A. Pádua, *J. Phys. Chem. B* **2006**, *110*, 19586–19592.
[84] R. Schurhammer, G. Wipff, *J. Phys. Chem. A* **2000**, *104*, 11159–11168.
[85] L. Martinez, R. Andrade, E. G. Birgin, J. M. Martinez, *J. Comb. Chem.* **2009**, *30*, 2157–2164.
[86] M. Brehm, B. Kirchner, *J. Chem. Inf. Model.* **2011**, *51*, 2007–2023.
[87] M. Brehm, M. Thomas, S. Gehrke, B. Kirchner, *J. Chem. Phys.* **2020**, *152*, 164105.

Manuscript received: November 22, 2022
Accepted manuscript online: January 19, 2023
Version of record online: February 7, 2023